

# Compound heterozygosity for loss-of-function *FARSB* variants in a patient with classic features of recessive aminoacyl-tRNA synthetase-related disease

Anthony Antonellis<sup>1,2,3</sup>  | Stephanie N. Oprescu<sup>1</sup> | Laurie B. Griffin<sup>3,4</sup> | Amer Heider<sup>5</sup> | Andrea Amalfitano<sup>6,7</sup> | Jeffrey W. Innis<sup>1,8</sup>

<sup>1</sup>Department of Human Genetics, University of Michigan Medical School, Ann Arbor, Michigan

<sup>2</sup>Department of Neurology, University of Michigan Medical School, Ann Arbor, Michigan

<sup>3</sup>Cellular and Molecular Biology Program, University of Michigan Medical School, Ann Arbor, Michigan

<sup>4</sup>Medical Scientist Training Program, University of Michigan Medical School, Ann Arbor, Michigan

<sup>5</sup>Department of Pathology, University of Michigan Medical School, Ann Arbor, Michigan

<sup>6</sup>Department of Pediatrics, College of Osteopathic Medicine, Michigan State University, East Lansing, Michigan

<sup>7</sup>Department of Microbiology and Molecular Genetics, Michigan State University, East Lansing, Michigan

<sup>8</sup>Department of Pediatrics, Division of Genetics, Metabolism, and Genomic Medicine, University of Michigan Medical School, Ann Arbor, Michigan

## Correspondence

Jeffrey W. Innis, 3737 Med Sci II, 1241 E. Catherine St. SPC 5618, Ann Arbor, MI 48109-5618.  
Email: innis@umich.edu

## Funding information

National Institute of Neurological Disorders and Stroke, Grant/Award Number: NS092238; National Institute of General Medical Sciences, Grant/Award Numbers: GM007315, GM007863, GM118647

Communicated by Garry R. Cutting

## Abstract

Aminoacyl-tRNA synthetases (ARSs) are ubiquitously expressed enzymes that ligate amino acids onto tRNA molecules. Genes encoding ARSs have been implicated in phenotypically diverse dominant and recessive human diseases. The charging of tRNA<sup>PHE</sup> with phenylalanine is performed by a tetrameric enzyme that contains two alpha (*FARSA*) and two beta (*FARSB*) subunits. To date, mutations in the genes encoding these subunits (*FARSA* and *FARSB*) have not been implicated in any human disease. Here, we describe a patient with a severe, lethal, multisystem, developmental phenotype who was compound heterozygous for *FARSB* variants: p.Thr256Met and p.His496Lysfs\*14. Expression studies using fibroblasts isolated from the proband revealed a severe depletion of both *FARSB* and *FARSA* protein levels. These data indicate that the *FARSB* variants destabilize total phenylalanyl-tRNA synthetase levels, thus causing a loss-of-function effect. Importantly, our patient shows strong phenotypic overlap with patients that have recessive diseases associated with other ARS loci; these observations strongly support the pathogenicity of the identified *FARSB* variants and are consistent with the essential function of phenylalanyl-tRNA synthetase in human cells. In sum, our clinical, genetic, and functional analyses revealed the first *FARSB* variants associated with a human disease phenotype and expand the locus heterogeneity of ARS-related human disease.

## KEYWORDS

aminoacyl-tRNA synthetase, developmental syndrome, *FARSB*, loss-of-function mutations, phenylalanyl-tRNA synthetase, recessive disease

Aminoacyl-tRNA synthetases (ARSs) are ubiquitously expressed enzymes that ligate tRNA molecules to cognate amino acids, which is the first step of protein translation (Antonellis & Green, 2008). Unsurprisingly, ablation of the function of any ARS enzyme in species ranging from mammals to bacteria is lethal, underscoring the essential role of these enzymes in cellular life. The human nuclear genome

contains 37 ARS-encoding loci, which together encode 17 enzymes required for tRNA charging in the mitochondria, 17 enzymes required for tRNA charging in the cytoplasm, and three enzymes that charge tRNA in both cellular compartments (Antonellis & Green, 2008). ARS enzymes are named according to the single-letter code of the amino acid they recognize followed by "ARS" and a variable "2" for

mitochondrial enzymes. For example, cytoplasmic tyrosyl-tRNA synthetase is referred to as “YARS,” whereas the corresponding mitochondrial enzyme is referred to as “YARS2” (Antonellis & Green, 2008).

To date, 31 ARS loci have been implicated in dominant and recessive human disease phenotypes (Meyer-Schuman & Antonellis, 2017). First, each of the 17 ARS loci encoding a mitochondrial enzyme has been implicated in recessive diseases and the vast majority are consistent with stereotypical mitochondrial disease phenotypes. Second, 13 of the 20 ARS loci encoding a cytoplasmic or bifunctional enzyme have been implicated in severe, early onset, developmental phenotypes with mostly overlapping features (Meyer-Schuman & Antonellis, 2017). Finally, five ARS loci encoding either a cytoplasmic or bifunctional enzyme have been implicated in dominant, axonal Charcot-Marie-Tooth disease (Antonellis et al., 2003; Jordanova et al., 2006; Latour et al., 2010; Tsai et al., 2017; Vester et al., 2012). Importantly, for the recessive diseases associated with ARS mutations, the inheritance patterns, nature of the mutations, functional studies, and significant phenotypic overlap associated with each locus all point to a loss-of-function mechanism (Meyer-Schuman & Antonellis, 2017; Oprescu, Griffin, Beg, & Antonellis, 2017).

The charging of tRNA molecules with phenylalanine in the cytoplasm is accomplished via a tetrameric enzyme that contains two catalytic subunits encoded by phenylalanyl-tRNA synthetase alpha (*FARSA*; MIM# 602918) and two regulatory subunits encoded by phenylalanyl-tRNA synthetase beta (*FARSB*; MIM# 609690) (Rodova, Ankilova, & Safro, 1999). To date, no variants in *FARSA* or *FARSB* have been implicated in human disease; however, loss-of-function mutations in the gene encoding mitochondrial phenylalanyl-tRNA synthetase (*FARS2*) have been implicated in recessive phenotypes including hereditary spastic paraplegia, Alpers syndrome, early onset epilepsy, global delay, dysarthria, and tremor (Almalki et al., 2014; Cho et al., 2017; Elo et al., 2012; Raviglione et al., 2016; Shamseldin et al., 2012; Vernon, McClellan, Batista, & Naidu, 2015; Walker et al., 2016; Yang et al., 2015). Here, we describe a patient with a severe, lethal, multisystem, developmental phenotype associated with compound heterozygosity for loss-of-function *FARSB* variants. Consent was obtained for this research, which was approved by the Institutional Review Board of the University of Michigan.

The male proband was born to a 31-year-old G2P0 mother at 35 and 4/7 weeks gestation and had a history of intrauterine growth restriction and oligohydramnios; his parents are nonconsanguineous. The family history was significant for a previous pregnancy loss at 37 weeks secondary to placental abruption. The proband was delivered by urgent cesarean section due to recurrent fetal heart rate with variable (and a few prolonged) decelerations. Apgar scores were 8 and 9 at 1 and 5 min, respectively. Birth weight was 1.927 kg (2%); length was 44 cm (8%); and head circumference was 32 cm (31%). Grunting was noted 10 min after birth, but with normal oximetry, and then recurred once at 5 hr after birth and resolved. The proband passed his newborn hearing and metabolic screens and pre- and post-ductal pulse oximetry. Physical examinations, other than being small for gestation age, were normal. He developed mild indirect hyperbilirubinemia on day of life 2 that responded to phototherapy appropriately. He was

discharged home and was initially bottle fed to gain weight, but was transitioned to breast feeding. He had frequent emesis greater than 20 min after feeds.

At 5 months (4 months corrected), his pediatrician referred him back to the University of Michigan for evaluation of failure to thrive, developmental delay, left inguinal hernia, tachypnea, and a chronic cough since birth occurring throughout the day and night. He was hospitalized for 2 months. Growth parameters had moved below the 3rd centile for weight and length and to 5th–10th centile for head circumference. Resting heart rate was in the 130 sec and he had baseline tachypnea (respiratory rate in the 70 sec). Physical examination was significant for sunken eyes, prominent cheeks, high palate, increased range of motion of joints, truncal hypotonia with marked head lag on pull to sit, and a small scrotum and phallus. Because of respiratory distress, he was transferred to the pediatric intensive care unit, where he required intubation for 4 days. Chest radiograph showed diffuse patchy airspace opacities with peribronchial cuffing. Multiple medical problems were identified including gastroesophageal reflux disease, profound vitamin D and A deficiency, severe hypocalcemia (requiring, at times, continuous calcium infusion up to 25 mg/kg/hr to maintain ionized calcium  $\geq 1.2$ ), supplementation with ergocalciferol or cholecalciferol, and hypoalbuminemia (albumin 2.4, protein 3.9) with anasarca and ascites, hungry bone syndrome with osteopenia and rickets, elevated liver transaminases (AST:100–300; ALT:80–150) and cholestasis (total bilirubin 3–4; direct bilirubin 2–3), yet normal INR. He had a nonanion gap metabolic acidosis, which resolved. CPK was 46, iron 39, ferritin 23.3, alpha-1-antitrypsin 173, and ceruloplasmin and cystic fibrosis sweat testing were normal. Numerous problems ensued during this hospitalization. He developed urinary tract infections with *Enterobacter cloacae* and *Enterococcus faecalis*, and had a normal VCUG. He also developed *Candida parapsilosis* bacteremia from his PICC line. He subsequently developed a DVT in the axillary vein above the PICC line. He had a seizure presumed secondary to hypoglycemia and hypocalcemia. Echocardiograms were performed on multiple occasions and revealed normal cardiac anatomy and good systolic function. Abdominal ultrasound revealed ascites without portal hypertension, as well as diffuse and increased parenchymal echogenicity suggestive of hepatocellular disease, and diffusely increased echogenicity of the kidneys, suggestive of renal disease. His abdominal distension improved after albumin infusion and he required diuretics for fluid overload. He did not have diarrhea and he had normal stool alpha-1-antitrypsin and stool elastase. He required post-pyloric tube feeds. Due to anemia and pancytopenia, a bone marrow biopsy was performed and flow cytometry was normal. He had a normal swallow study. MRI of the abdomen revealed hepatic steatosis but no increased liver iron. Hepatitis viral serologies were negative. Head ultrasound identified possible abnormal periventricular white matter and bilateral basal ganglia echogenicity, and follow-up brain MRI at 5 months corrected age, showed cerebral volume loss and incomplete closure of the Sylvian fissures (Figure 1A and B); MR spectroscopy showed no lactate peak. Myelination was appropriate for age given his prematurity. He had an episode of dysconjugate gaze and abnormal tracking eye movements and was found to have hypoglycemia to 37 mg/dl after being fasted for 2.5 hr in preparation for a fasting blood specimen; at that time head CT and MRI

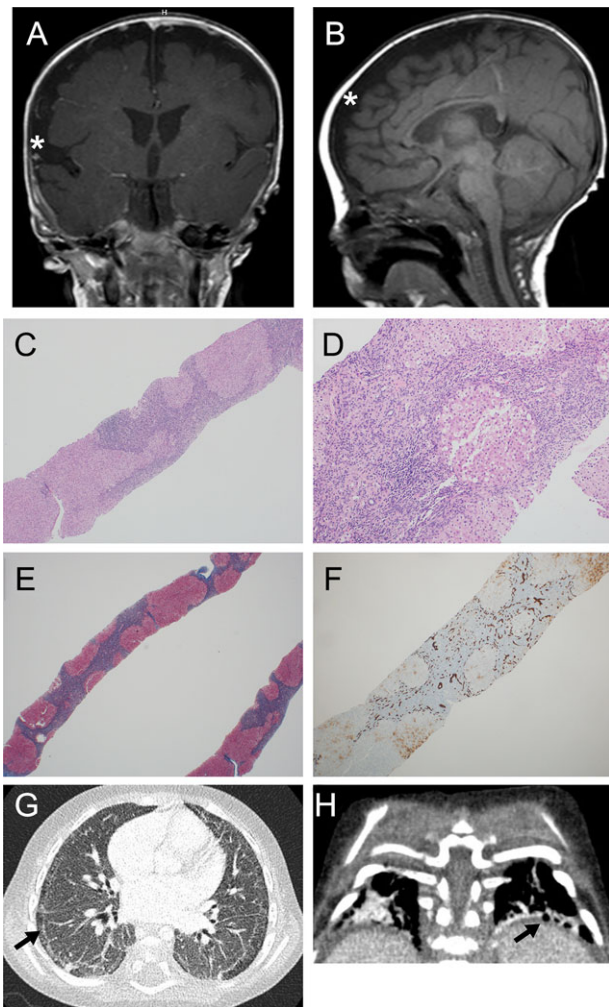


**FIGURE 1** Head MRI, liver pathology, and chest CT of the proband. **A and B:** Coronal and sagittal T1-weighted head MRI images obtained at 5 months corrected age showing incomplete closure of the Sylvian fissures (asterisk in **A**), and bilateral frontoparietal cerebral volume loss (asterisk in **B**). **C–F:** Liver pathology. Architectural distortion (4 $\times$ ) with nodular formation (**C**); portal chronic inflammation with focal steatosis (10 $\times$ ) (**D**); Masson trichrome stain (2 $\times$ ) with well-developed cirrhosis and bridging fibrosis (**E**); and CK7 immunostain (4 $\times$ ) showing extensive bile ductular reaction (**F**). **G and H:** Chest CT (18 months) showing subpleural cystic changes (arrows) and interstitial disease

were nonspecific. One week later, he had a seizure-like event with left upward eye gaze and symmetric jerking of all extremities associated with ionized calcium of 0.88 mmol/l, which responded to supplementation. He developed worsening tachypnea with increasing ascites, usually associated with hypoalbuminemia (a chronic problem during and after this hospitalization). After extubation, he was placed on CPAP and then weaned to high flow nasal cannula and then room air over the course of a week. He remained intermittently tachypneic. He was discharged after 2 months (corrected age 6 months) and had a heart rate of 150–160 per minute, respiratory rate of  $\sim$ 40 per minute, discharge weight 4.86 kg ( $\ll$  3%; 50% for a 1.5 month old), length 60 cm ( $<$ 3%; 50% for a 2.75 month old), and head circumference 42 cm (10%).

Interstitial pulmonary disease, liver cirrhosis (hypoalbuminemia), and portal hypertension with ascites, esophageal varices with GI

bleeding, developmental delay, and failure to thrive continued to be problems. G-tube placement and percutaneous left lobe liver biopsy were performed at 14 months. The liver parenchyma showed architectural distortion with nodular formation and bridging fibrosis by trichrome (Figure 1C and E). Focal mild steatosis was observed (Figure 1D). CK7 immunostaining revealed bile ductular proliferation (Figure 1F). Moderate chronic portal inflammatory infiltrates were noted with neutrophils associated with the ductular reaction. There is patchy intrahepatocyte cholestasis, without significant intracanalicular cholestasis or bile plugging. No clear lobular hepatic pattern or interface activity (such as plasma cells at the limiting plate) was appreciated. Iron stain was negative. There were no viral cytopathic effects identified. The overall findings were consistent with well-established cirrhosis of unknown etiology. Electron microscopy (Supp. Figure S1) was performed and hepatocytes showed reactive expansion of smooth ER, focal cystic dilation of rough ER containing sparse delicate material of no specific appearance, focal accumulation of glycogen granules, common autophagic bodies, bulky accumulations of non-membrane bound material consistent with bile residue in hepatocyte cytoplasm, and universally normal appearing mitochondria. Many hepatocytes contained abundant microvesicular lipid that appeared to be nonmembrane bound and thus free in the cytoplasm. No abnormal storage of material was identified within the lysosomes or cytoplasm.

Chest CT at 1.5 years and chest radiographs at 22 months, showed subpleural cystic changes in the bilateral lungs consistent with interstitial lung disease (Figure 1G and H). Bronchoscopy showed only moderate dynamic collapse in the left main stem and lingual regions; milder collapse in the LLL segments. Bronchoalveolar lavage was negative for alveolar proteinosis and malignancy. Because of the pulmonary findings, a left nasal brushing biopsy was performed and showed motile cilia, and electron microscopy revealed normal respiratory ciliary ultrastructure. He was found to have pulmonary hypertension at 22 months at the time of an acute respiratory exacerbation requiring high frequency oscillatory ventilation, milrinone, and inhaled nitrous oxide. At that time, he had a normal bubble study negative for hepatopulmonary syndrome and normal biventricular function. He developed a subacute DVT in the distal external iliac and common femoral veins and was anticoagulated. He developed a right-sided intraparenchymal brain hemorrhage, presumed secondary to lovenox therapy. He received a ventriculostomy at 23 months; continued bleeding was noticed in the right parietal region. He developed hydrocephalus, which worsened with intraparenchymal hemorrhage and ultimately received a VP shunt at 24 months.

Medical Genetics consultation revealed normal results for N-glycan and O-glycan profiles, CPK, lysosomal enzymes including acid maltase, quantitative plasma and CSF amino acids, very long chain fatty acids, acylcarnitine profiles, SNP-based chromosomal microarray, methylation PCR for Prader-Willi/Angelman syndromes, 7-dehydrocholesterol, and *ATP7A* (MIM# 300011) sequencing. Urine organic acid analysis revealed 4-hydroxyphenylacetic, 4-hydroxyphenylactic, and 4-hydroxyphenylpyruvate, consistent with liver dysfunction. Right thigh skeletal muscle biopsy by standard histological analysis showed nonspecific findings with slightly increased lipid droplets within fibers. Transmission electron microscopy showed

nonspecific, mild mitochondrial and myofibrillar irregularities. Muscle mitochondrial electron transport chain (ETC) enzyme analysis demonstrated increased citrate synthase (CS) control enzyme activity, with deficiency (15% of control after normalization for CS activity) of rotenone sensitive complex I + III activity, fulfilling one major modified Walker criterion for the diagnosis of a respiratory chain disorder. Several other ETC activities were reduced with relative preservation of complex II. Venous and arterial lactate was measured multiple times and was not consistently elevated. Because of the enzyme deficiencies noted, a 164 nuclear gene and mitochondrial next-generation sequencing panel was obtained at 24 months. This analysis revealed heterozygosity for a maternally inherited *NDUFS2* (MIM# 602985) variant of uncertain significance (VUS), p.H380D (a variant with a frequency of 0.15% in the NHLBI ESP and 0.06% in ExAC, with no homozygotes), and hemizyosity for a maternally inherited *PHKA2* (MIM# 300798) VUS, p.L413S (not seen in ESP; 0.008% in ExAC with 5 hemizygotes) (Lek et al., 2016). No second variant was identified in *NDUFS2*, which would be required to consider this recessive disorder (Loeffen et al., 2001). *PHKA2* deficiency is unlikely as there was no liver glycogenesis observed on biopsy and the other clinical features of the proband are much more severe than typical patients with this disorder (Hendrickx et al., 1995). Thus, neither the *NDUFS2* nor *PHKA2* variants accounted for the severe clinical manifestations of the proband, who was readmitted multiple times for respiratory failure and hypoalbuminemia requiring intensive care, and passed away at 32 months. No autopsy was obtained.

To further explore the genetic underpinnings of the phenotype identified in our proband, we performed whole-exome sequencing (WES) analysis on DNA isolated from blood from the proband and his unaffected parents. Trio WES studies performed at GeneDx (Gaithersburg, MD) revealed the aforementioned maternally inherited variants of unknown significance in *NDUFS2* and *PHKA2*. The only other candidate pathogenic variants identified in these studies that met the inheritance pattern and allele frequency criteria were two variants of unknown significance in *FARSB*: c.767C > T, which predicts a p.Thr256Met missense variant; and c.1486delCinsAA, which predicts a p.His496Lysfs\*14 protein-truncating or null allele. The unaffected father is heterozygous for p.Thr256Met, the unaffected mother is heterozygous for p.His496Lysfs\*14, and the proband was compound heterozygous for both *FARSB* variants (Figure 2A). Please note that these variants are annotated on NM\_005687.4 and each was validated using Mutalyzer (<https://mutalyzer.nl>). The variants and associated phenotype have been submitted to ClinVar (<https://www.ncbi.nlm.nih.gov/clinvar/>): p.Thr256Met accession no. SCV000676382; p.His496Lysfs\*14 accession no. SCV000676381.

Examination of each *FARSB* variant on the genome aggregate database browser (gnomAD; <https://gnomad.broadinstitute.org>) (Lek et al., 2016) revealed the presence of p.Thr256Met *FARSB* at a very low frequency (12 out of 276,122 alleles with no homozygous individuals) and the absence of p.His496Lysfs\*14 *FARSB*. While p.His496Lysfs\*14 *FARSB* is very likely to result in a null allele or a nonfunctional protein, the importance of p.Thr256 in enzyme function is less clear. Multiple-species conservation analysis revealed that p.Thr256 is conserved among diverse species ranging from human to yeast (Fig-

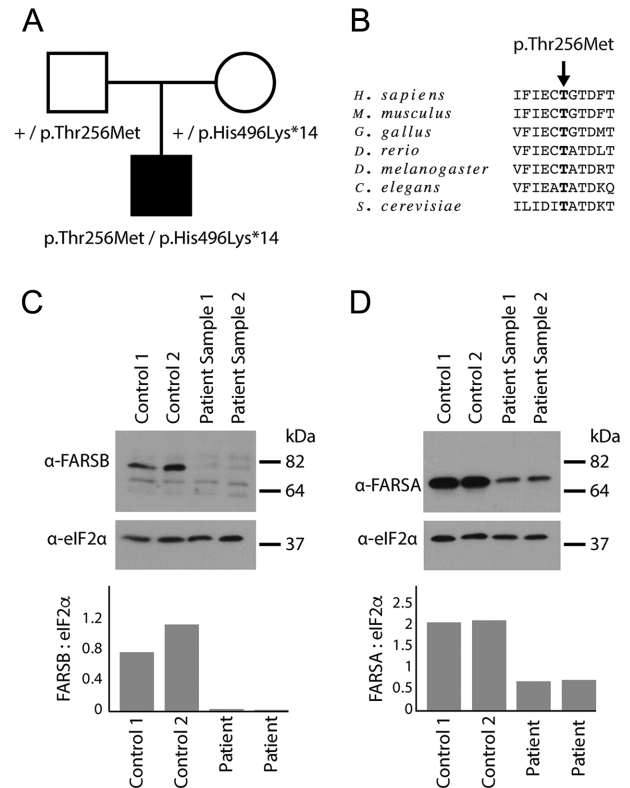


**FIGURE 2** Characterization of the *FARSB* variants identified in the proband. **A:** A simplex pedigree is shown with squares representing males and circles representing females. Genotypes are indicated under each symbol for the father, mother, and male proband (filled square). The proband is the only affected individual in the pedigree. **B:** The position of the p.Thr256Met variant is shown along with surrounding amino acid sequences for multiple, evolutionarily diverse species. Species are indicated along the left and the position of the affected residue is indicated by an arrow and bold text. **C:** Western blot analyses were performed using total protein lysates from fibroblasts isolated from two control individuals and from the patient described in this study, the latter performed in duplicate (Sample 1 and Sample 2). An anti-FARSB or anti-eIF2 $\alpha$  antibody was employed to test for the effect of the *FARSB* variants on protein levels and to control for protein loading, respectively. Sample names are provided across the top of the panel and sizes in kDa are indicated on the right. **D:** Similar western blot analyses as described in panel C using an anti-FARSA antibody. In panels C and D, the ratio of FARSB or FARSA to eIF2 $\alpha$  was determined by dividing the optical density of each FARS-specific band by that of the corresponding eIF2 $\alpha$ -specific band

ure 2B). Furthermore, resolving the structure of human cytoplasmic phenylalanyl-tRNA synthetase revealed that threonine 256 resides in the editing domain and mutating this residue to alanine reduces the ability to distinguish between tyrosine and phenylalanine, resulting in enzyme mischarging (Finarov, Moor, Kessler, Klipcan, & Safro, 2010; Sasaki et al., 2006).

Since p.His496Lysfs\*14 *FARSB* causes a frameshift mutation that leads to a premature stop codon, the variant is predicted to ablate the expression of full-length *FARSB*, which would predict a ~50% decrease in full-length protein levels in patient cells. To address this, we performed western blot analysis on proteins isolated from cultured patient fibroblasts and two control fibroblast lines (i.e., from

individuals without *FARSB* variants). Briefly, protein samples (20  $\mu$ g per sample) were subjected to electrophoresis, transferred onto a PVDF membrane, and incubated with an anti-*FARSB* antibody (Sigma-Aldrich, St. Louis, MO; HPA061398) or an anti-eIF2 $\alpha$  antibody (Cell Signaling Technology, Danvers, MA; 9722) to control for protein loading. Interestingly, our results revealed a dramatic reduction of full-length *FARSB* protein levels (~97% reduction) in patient fibroblast cells compared to control cell lines (Figure 2C). Since *FARSB* forms an  $\alpha_2\beta_2$  hetero-tetramer with *FARSA* (Rodova et al., 1999), we hypothesized that severely reduced *FARSB* levels may destabilize and reduce *FARSA* levels. To address this, we performed the same western blot analyses described above using an antibody designed against *FARSA* (Sigma-Aldrich, St. Louis, MO; HPA001911). These analyses revealed a significant decrease in *FARSA* levels (~66% reduction) in patient cells compared to the control cell lines (Figure 2D).

The observation of dramatically reduced *FARSB* protein levels in patient cells requires further consideration of the p.Thr256Met *FARSB* missense variant. We computationally predicted the pathogenicity of this variant using CADD (Kircher et al., 2014), PolyPhen2 (Adzhubei et al., 2010), and MUPro (Cheng, Randall, & Baldi, 2006), and all three algorithms provided a prediction of "pathogenic": CADD score = 33; PolyPhen2 score = 1; and MUPro score = -0.4315118. Importantly, MUPro scores that are less than 0 predict a decrease in protein stability that is consistent with our western blot analyses. Thus, even though p.Thr256Met *FARSB* resides in the editing domain (see above), this variant likely impacts protein stability that would result in reduced tRNA charging. Indeed, the lack of a phenotype in the father that carries p.Thr256Met *FARSB* and previous reports showing that Chinese hamster ovary cells are tolerant of misincorporations of phenylalanine for tyrosine (Raina et al., 2014) indicate that altered editing is not likely to be responsible for the phenotype observed in the proband. We therefore conclude that compound heterozygosity for p.Thr256Met and p.His496Lysfs\*14 *FARSB* results in a severe reduction of *FARSB* protein levels that causes a downstream reduction in *FARSA* levels. These reduced protein levels likely result in a severe reduction in phenylalanyl-tRNA synthetase activity that is responsible for the observed recessive disease phenotype in our patient. In support of this notion, we are aware of another family with two affected siblings, both with novel, bi-allelic *FARSB* variants including a predicted loss-of-function variant and a predicted deleterious missense variant, and very similar clinical features (Wendy Chung, personal communication).

A detailed comparison of the phenotypes of our proband (described above) and the phenotypes of previously reported patients with ARS-associated recessive disease (Meyer-Schuman & Antonellis, 2017) revealed striking overlap (Supp. Table S1). For example, the following phenotypes that we observed in our patient have been reported in patients with other ARS-associated recessive syndromes: (1) intrauterine growth restriction in patients with AARS (MIM# 601065), GARS (MIM# 600287), IARS (MIM# 600709), MARS (MIM# 156560), MARS2 (MIM# 609728), QARS (MIM# 603727), VARS (MIM# 192150), and YARS2 (MIM# 610957) variants; (2) failure to thrive in patients with AARS, AARS2 (MIM# 612035), CARS2 (MIM# 612800), EARS2 (MIM# 612799), IARS, LARS (MIM# 151350), MARS, MARS2, SARS2 (MIM# 612804), YARS (MIM# 603623), and YARS2 variants; (3)

developmental delay in patients with AARS, *FARS2* (MIM# 611592), GARS, IARS, KARS (MIM# 601421), LARS, MARS, MARS2, NARS2 (MIM# 612803), PARS2 (MIM# 612036), QARS, RARS2 (MIM# 611524), SARS2, VARS, and YARS variants; (4) hypotonia in patients with CARS2, EARS2, HARS2 (MIM# 600783), IARS, KARS, LARS, MARS, MARS2, QARS, RARS (MIM# 107820), RARS2, SARS2, TARS2 (MIM# 612805), and YARS variants; (5) abnormal or decreased white matter in patients with AARS, CARS2, DARS (MIM# 603084), DARS2 (MIM# 610956), EARS2, GARS, IARS, KARS, MARS2, NARS2, QARS, RARS, RARS2, and YARS variants; and (6) liver dysfunction in patients with EARS2, *FARS2*, IARS, LARS, LARS2 (MIM# 604544), MARS, and YARS variants.

In addition to the overlap with individual features of other ARS-related recessive syndromes, the phenotype of our patient displayed remarkable overlap with features previously associated with homozygosity or compound heterozygosity for loss-of-function methionyl-tRNA synthetase (*MARS*) variants including: intrauterine growth restriction; failure to thrive; developmental delay; inguinal hernia; hypotonia; recurrent infections; interstitial lung disease; and liver dysfunction (van Meel et al., 2013; Hadchouel et al., 2015; Sun et al., 2017). Similarly, our patient shared many clinical features previously associated with homozygosity or compound heterozygosity for loss-of-function tyrosyl-tRNA synthetase (*YARS*) variants including: intrauterine growth restriction; failure to thrive; developmental delay; emesis; deep-set eyes; prominent cheeks; high palate; joint hypermobility; hypotonia; abnormal white matter; and liver dysfunction (Nowaczyk et al., 2017; Tracewska-Siemiątkowska et al., 2017). Importantly, the phenotypic overlap between our patient and other patients with recessive ARS-related diseases strongly supports the pathogenicity of the *FARSB* variants reported here. Furthermore, this phenotypic overlap also indicates that the mutations have a direct effect on the primary function of the enzyme: charging tRNA with phenylalanine for protein translation. In support of this latter notion, many of the clinical manifestations reported here have been associated with mutations that disrupt the cytoplasmic or mitochondrial protein translational machinery (Scheper, van der Knaap, & Proud, 2007), including liver dysfunction—arguably the most severe phenotype observed in our patient—associated with *EIF2AK3* (MIM# 604032), *GFM1* (MIM# 606639), *TUFM* (MIM# 602389), and *GCN2* (MIM# 609280) perturbations (Coenen et al., 2004; Delépine et al., 2000; Guo & Cavener, 2007; Valente et al., 2007).

In summary, we describe clinical, genetic, and functional data that implicate *FARSB* mutations in a severe, lethal, multisystem, recessive, and developmental phenotype. These data warrant careful assessments for loss-of-function *FARSB*—or *FARSA*—variants in patients with a similar clinical syndrome, especially when liver dysfunction is described. Our study expands the locus heterogeneity of diseases associated with ARSs (Meyer-Schuman & Antonellis, 2017) and emphasizes the importance of detailed clinical comparisons and relevant functional studies when implicating ARS variants in disease pathogenesis (Oprescu et al., 2017).

## ACKNOWLEDGMENTS

The authors thank the family for their patience and involvement in the study, and their interest and dedication to this research. We also wish

to acknowledge the efforts of a large army of physicians, nurses, and other caretakers in the life of this patient. Finally, we thank Dr. Doug Quint for help with the head MRI interpretation and Dr. Wendy Chung for sharing knowledge of a second family with *FAR5B* variants. J.W.I. would like to acknowledge support from the Morton S. and Henrietta K. Sellner Professorship in Human Genetics. A. Amalfitano acknowledges the Osteopathic Heritage Foundation and the Michigan State University Foundation for support.

## DISCLOSURE STATEMENT

The authors declare no conflict of interest.

## ORCID

Anthony Antonellis  <http://orcid.org/0000-0002-5820-3156>

## REFERENCES

- Adzhubei, I. A., Schmidt, S., Peshkin, L., Ramensky, V. E., Gerasimova, A., Bork, P., ... Sunyaev, S. R. (2010). A method and server for predicting damaging missense mutations. *Nature Methods*, *7*, 248–249.
- Almalki, A., Alston, C. L., Parker, A., Simonic, I., Mehta, S. G., He, L., ... Chrzanowska-Lightowlers, Z. M. (2014). Mutation of the human mitochondrial phenylalanine-tRNA synthetase causes infantile-onset epilepsy and cytochrome c oxidase deficiency. *Biochimica et Biophysica Acta*, *1842*, 56–64.
- Antonellis, A., Ellsworth, R. E., Sambuughin, N., Puls, I., Abel, A., Lee-Lin, S-Q., ... Green, E.D. (2003). Glycyl tRNA synthetase mutations in Charcot-Marie-Tooth disease type 2D and distal spinal muscular atrophy type V. *American Journal of Human Genetics*, *72*, 1293–1299.
- Antonellis, A., & Green, E. D. (2008). The role of aminoacyl-tRNA synthetases in genetic diseases. *Annual Review of Genomics and Human Genetics*, *9*, 87–107.
- Cheng, J., Randall, A., & Baldi, P. (2006). Prediction of protein stability changes for single-site mutations using support vector machines. *Proteins*, *62*, 1125–1132.
- Cho, J. S., Kim, S. H., Kim, H. Y., Chung, T., Kim, D., Jang, S., ... Lim, B. C. (2017). *FARS2* mutation and epilepsy: Possible link with early-onset epileptic encephalopathy. *Epilepsy Research*, *129*, 118–124.
- Coenen, M. J., Antonicka, H., Ugalde, C., Sasarman, F., Rossi, R., Heister, J. G., ... Smeitink, J. A. (2004). Mutant mitochondrial elongation factor G1 and combined oxidative phosphorylation deficiency. *New England Journal of Medicine*, *351*, 2080–2086.
- Delépine, M., Nicolino, M., Barrett, T., Golamaully, M., Lathrop, G. M., & Julier, C. (2000). EIF2AK3, encoding translation initiation factor 2-alpha kinase 3, is mutated in patients with Wolcott-Rallison syndrome. *Nature Genetics*, *25*, 406–409.
- Elo, J. M., Yadavalli, S. S., Euro, L., Isohanni, P., Götz, A., Carroll, C. J., ... Suomalainen A. (2012). Mitochondrial phenylalanyl-tRNA synthetase mutations underlie fatal infantile Alpers encephalopathy. *Human Molecular Genetics*, *21*, 4521–4529.
- Finarov, I., Moor, N., Kessler, N., Klipcan, L., & Saftro, M. G. (2010). Structure of human cytosolic phenylalanyl-tRNA synthetase: Evidence for kingdom-specific design of the active sites and tRNA binding patterns. *Structure (London, England)*, *18*, 343–353.
- Guo, F., & Cavener, D. R. (2007). The GCN2 eIF2alpha kinase regulates fatty-acid homeostasis in the liver during deprivation of an essential amino acid. *Cell Metabolism*, *5*, 103–114.
- Hadchouel, A., Wieland, T., Griese, M., Baruffini, E., Lorenz-Depiereux, B., Enaud, L., ... Strom T.M. (2015). Biallelic mutations of methionyl-tRNA synthetase cause a specific type of pulmonary alveolar proteinosis prevalent on Réunion Island. *American Journal of Human Genetics*, *96*, 826–831.
- Hendrickx, J., Coucke, P., Dams, E., Lee, P., Odièvre, M., Corbeel, L., ... Willems, P. J. (1995). Mutations in the phosphorylase kinase gene PHKA2 are responsible for X-linked liver glycogen storage disease. *Human Molecular Genetics*, *4*, 77–83.
- Jordanova, A., Irobi, J., Thomas, F. P., Van Dijck P., Meerschaert, K., Dewil, M., ... Timmerman V. (2006). Disrupted function and axonal distribution of mutant tyrosyl-tRNA synthetase in dominant intermediate Charcot-Marie-Tooth neuropathy. *Nature Genetics*, *38*, 197–202.
- Kircher, M., Witten, D. M., Jain, P., O’Roak, B. J., Cooper, G. M., & Shendure, J. (2014). A general framework for estimating the relative pathogenicity of human genetic variants. *Nature Genetics*, *46*, 310–315.
- Latour, P., Thauvin-Robinet, C., Baudalet-Méry, C., Soichot, P., Cusin, V., Faivre, L., ... Rousson R. (2010). A major determinant for binding and aminoacylation of tRNA(Ala) in cytoplasmic Alanyl-tRNA synthetase is mutated in dominant axonal Charcot-Marie-Tooth disease. *American Journal of Human Genetics*, *86*, 77–82.
- Lek, M., Karczewski, K. J., Minikel, E. V., Samocha, K. E., Banks, E., Fennell, T., ... Birnbaum, D. P., Exome Aggregation Consortium (2016). Analysis of protein-coding genetic variation in 60,706 humans. *Nature*, *536*, 285–291.
- Loeffen, J., Elpeleg, O., Smeitink, J., Smeets, R., Stöckler-Ipsiroglu, S., Mandel, H., ... van den Heuvel, L. (2001). Mutations in the complex I *NDUFS2* gene of patients with cardiomyopathy and encephalomyopathy. *Annals of Neurology*, *49*, 195–201.
- Meyer-Schuman, R., & Antonellis, A. (2017). Emerging mechanisms of aminoacyl-tRNA synthetase mutations in recessive and dominant human disease. *Human Molecular Genetics*, *26*, R114–R127.
- Nowaczyk, M. J., Huang, L., Tarnopolsky, M., Schwartzentruber, J., Majewski, J., Bulman, D. E., ... Boycott, K. M. (2017). A novel multisystem disease associated with recessive mutations in the tyrosyl-tRNA synthetase (YARS) gene. *American Journal of Medical Genetics. Part A*, *173*, 126–134.
- Oprescu, S. N., Griffin, L. B., Beg, A. A., & Antonellis, A. (2017). Predicting the pathogenicity of aminoacyl-tRNA synthetase mutations. *Methods (San Diego, California)*, *113*, 139–151.
- Raina, M., Moghal, A., Kano, A., Jerums, M., Schnier, P. D., Luo, S., ... Ibba, M. (2014). Reduced amino acid specificity of mammalian tyrosyl-tRNA synthetase is associated with elevated mistranslation of Tyr codons. *Journal of Biological Chemistry*, *289*, 17780–17790.
- Ravignone, F., Conte, G., Ghezzi, D., Parazzini, C., Righini, A., Vergaro, R., ... Mastrangelo, M. (2016). Clinical findings in a patient with *FARS2* mutations and early-infantile-encephalopathy with epilepsy. *American Journal of Medical Genetics. Part A*, *170*, 3004–3007.
- Rodova, M., Ankilova, V., & Saftro, M. G. (1999). Human phenylalanyl-tRNA synthetase: Cloning, characterization of the deduced amino acid sequences in terms of the structural domains and coordinately regulated expression of the alpha and beta subunits in chronic myeloid leukemia cells. *Biochemical and Biophysical Research Communications*, *255*, 765–773.
- Sasaki, H. M., Sekine, S-I., Sengoku, T., Fukunaga, R., Hattori, M., Utsunomiya, Y., ... Yokoyama, S. (2006). Structural and mutational studies of the amino acid-editing domain from archaeal/eukaryal phenylalanyl-tRNA synthetase. *Proceedings of the National Academy of Sciences of the United States of America*, *103*, 14744–14749.
- Scheper, G. C., van der Knaap, M. S., & Proud, C. G. (2007). Translation matters: Protein synthesis defects in inherited disease. *Nature Reviews Genetics*, *8*, 711–723.

- Shamseldin, H. E., Alshammari, M., Al-Sheddi, T., Salih, M. A., Alkhalidi, H., Kentab, A., ... Alkuraya, F. S. (2012). Genomic analysis of mitochondrial diseases in a consanguineous population reveals novel candidate disease genes. *Journal of Medical Genetics*, *49*, 234–241.
- Sun, Y., Hu, G., Luo, J., Fang, D., Yu, Y., Wang, X., ... Qiu, W. (2017). Mutations in methionyl-tRNA synthetase gene in a Chinese family with interstitial lung and liver disease, postnatal growth failure and anemia. *Journal of Human Genetics*, *48*, 337.
- Tracewska-Siemiatkowska, A., Haer-Wigman, L., Bosch, D. G. M., Bamshad M.J., University of Washington Center for Mendelian Genomics, van de Vorst, M., ... Tranebjærg L. (2017) An expanded multi-organ disease phenotype associated with mutations in YARS. *Genes (Basel)*, *8*, 381.
- Tsai, P-C, Soong, B-W, Mademan, I, Huang, Y-H, Liu, C-R, Hsiao, C-T, ... Lee, Y. C. (2017). A recurrent WARS mutation is a novel cause of autosomal dominant distal hereditary motor neuropathy. *Brain*, *140*:1252–1266.
- Valente, L., Tiranti, V., Marsano, R. M., Malfatti, E., Fernandez-Vizarra, E., Donnini, C., ... Zeviani M. (2007). Infantile encephalopathy and defective mitochondrial DNA translation in patients with mutations of mitochondrial elongation factors EFG1 and EFTu. *American Journal of Human Genetics*, *80*, 44–58.
- van Meel E., Wegner, D. J., Cliften, P., Willing, M. C., White, F. V., Kornfeld, S., & Cole, F. S. (2013). Rare recessive loss-of-function methionyl-tRNA synthetase mutations presenting as a multi-organ phenotype. *BMC Medical Genetics [Electronic Resource]*, *14*, 106.
- Vernon, H. J., McClellan, R., Batista, D. A., & Naidu, S. (2015). Mutations in FARS2 and non-fatal mitochondrial dysfunction in two siblings. *American Journal of Medical Genetics. Part A*, *167A*, 1147–1151.
- Vester, A., Velez-Ruiz, G., McLaughlin, H. M., NISC Comparative Sequencing Program, Lupski, J. R., Talbot, K., Vance, J. M., Züchner, S., Roda, R. H., Fischbeck, K. H., ... Antonellis A. (2012). A loss-of-function variant in the human histidyl-tRNA synthetase (HARS) gene is neurotoxic in vivo. *Human Mutation*, *34*, 191–199.
- Walker, M. A., Mohler, K. P., Hopkins, K. W., Oakley, D. H., Sweetser, D. A., Ibba, M., ... Thibert, R. L. (2016). Novel compound heterozygous mutations expand the recognized phenotypes of FARS2-linked disease. *Journal of Child Neurology*, *31*, 1127–1137.
- Yang, Y., Liu, W., Fang, Z., Shi, J., Che, F., He, C., ... Wu, Y. (2015). A newly identified missense mutation in FARS2 causes autosomal-recessive spastic paraplegia. *Human Mutation*, *37*, 165–169.

## SUPPORTING INFORMATION

Additional Supporting Information may be found online in the supporting information tab for this article.

**How to cite this article:** Antonellis A, Oprescu SN, Griffin LB, Heider A, Amalfitano A, Innis JW. Compound heterozygosity for loss-of-function *FARSB* variants in a patient with classic features of recessive aminoacyl-tRNA synthetase-related disease. *Human Mutation*. 2018;39:834–840. <https://doi.org/10.1002/humu.23424>